

Eigenvalue Decomposition of Meson Correlators

Thomas DeGrand

Department of Physics, University of Colorado, Boulder, CO 80309 USA

(Dated: October 29, 2018)

Euclidean space hadronic correlators are computed in quenched QCD at small quark mass using truncations of quark propagators which include or exclude low eigenvalue eigenmodes of the Dirac operator. High modes provide the dominant contribution to parity averaged correlators, especially at short distances. Differences of correlators of opposite parity receive most of their contributions from low modes and are much smaller in size than parity averages at short distances. The pion propagator in any correlator to which it couples receives a large contribution from low modes, while the tensor meson correlator receives a tiny contribution from low eigenmodes.

I. INTRODUCTION

Are all hadrons alike? This question was asked most famously [1] in the context of QCD sum rules, but it appears repeatedly in phenomenological descriptions of hadronic structure. In this work I investigate a particular kind of similarity: how eigenmodes of the 4-dimensional Dirac operator contribute to Euclidean space hadronic correlators, and so (indirectly) how these eigenmodes contribute to hadronic spectroscopy and couplings in different channels. My results might have implications for the questions of whether excited states of mesons show features of chiral symmetry restoration (namely, that the masses of various states, and their couplings to currents, show degeneracies), what the origin of these features might be, and how excited states differ from low lying meson states.

Lattice simulations encode “snapshots” of the QCD vacuum, and could presumably address questions about the composition of hadronic states. This subject has been investigated before [2, 3]. The idea is to compare the behavior of hadronic correlators built from quark propagators which correspond to a truncated set of eigenmodes of the massless Dirac operator with that of correlators computed “exactly.” Low eigenmodes of the Dirac operator saturate the pseudoscalar and axial vector correlators at large distance and contribute somewhat to the nucleon channel, less so the vector and Delta channels. They also make the dominant contribution to the eta-prime channel, as expected from the Witten-Veneziano formula [4]. In this work I revisit these studies, with an eye toward contrasting the Dirac eigenmode composition of the long-distance part of hadronic correlators with the short-distance parts, as well as the composition of correlators which are sums and differences of parity partners (γ_5 and 1, γ_i and $\gamma_i\gamma_5$). All these calculations reveal the following qualitative features of mesons in quenched QCD: Low eigenmodes of the Dirac operator do not affect the part of correlators where high-lying states appear. These low modes are the ones which determine the quark condensate via the Banks-Casher [5] relation, as well as eigenmodes “at the QCD scale” (a few hundred MeV). Other ways of describing the properties of low modes are that they are strongly influenced by chirality-mixing interactions, and that they are the main contributors to the strong interaction observed in the pseudoscalar current-current correlator.

High modes contribute strongly to hadron correlators at short distance, where the correlators would be dominated by excited states. They contribute less to the long distance part of meson correlators. They do not make a major contribution to parity asymmetric correlators. In this sense, valence quarks in high-lying states decouple from the condensate. This also means that even for light quarks, chiral symmetry breaking and confinement are not directly related. These observations are rather simple, and perhaps one does not “need” lattice simulations to see them. I suspect that no phenomenologist will find them surprising (although I suspect that different phenomenologists will be unsurprised for different reasons.) Instanton models plus lattice simulations have also been used to compute the amplitude for chiral mixing of $q\bar{q}$ correlators [6, 7]. Ref. [2] also observed that the lowest eigenvalue modes had a large autocorrelation in both density and chirality at short distance, which slowly dies away as the eigenmode rises.

Analyses of hadronic spectroscopy [8, 9, 10, 11, 12, 13, 14] have been used to argue that excited states of the meson and baryon spectrum are effectively chirally restored, in the sense that particles of opposite parity are nearly degenerate in mass. It is argued that this “effective restoration of chiral symmetry” is a natural consequence of the soft nature of chiral symmetry breaking: generally in quantum mechanics, low excitations are sensitive to symmetry breaking but high excitations are not. For mesons, the crossover to chiral symmetry is argued to occur in the range 1.5-2 GeV.

In perturbation theory, correlators of currents which are chiral partners of each other (the vector and axial vector currents, for example) are identical, because QCD is a vector theory and chirality is conserved at all quark-gluon vertices. Condensates allow one to parameterize nonperturbative physics, and can lead to differences in correlators. However, QCD is a confining theory, and the spectrum of QCD is one of bound states, so identity of the correlators must have consequences for spectroscopy and matrix elements. That is especially true for the large- N_c limit of QCD,

where all excitations are narrow resonances. Arguments based on semi-local duality favoring effective chiral restoration at high excitation have been made [15]. but have been criticised as being cutoff dependent[16].

A summary of ideas supporting chiral restoration and its connection to the quark model has recently been given by Swanson[17].

In instanton models[18] low eigenmodes of the Dirac operator are built from an overlap of single-instanton zero modes, and are strongly chirally asymmetric. As the magnitude of the quark eigenmode rises, the eigenfunctions couple less and less to instantons, and there should be a ‘‘crossover’’ to chirally-symmetric physics.

The common lattice correlators used to extract spectroscopy involve projections onto momentum eigenstates. For example, the $\vec{p} = 0$ correlator is found by averaging over time slices:

$$\begin{aligned} C_j(t) &= \sum_x \langle 0 | O_j(x, t) O_j(0, 0) | 0 \rangle \\ &= \sum_n \frac{\langle 0 | O_j | n \rangle^2}{2m_n} \exp(-m_n t) \end{aligned} \tag{1}$$

A second kind of observable is just the point-to-point correlator

$$\Pi_i(x) = \text{Tr} \langle J_i^a(x) J_i^a(0) \rangle, \tag{2}$$

where the current will be proportional to $J_i^a(x) = \bar{\psi}(x) \tau^a \Gamma(i) \psi(x)$, and its ratio to the free-field correlator $R_i(x) = \Pi_i(x) / \Pi_i^0(x)$. It is very difficult to compute masses of highly excited states from lattice simulations. Their signals vanish exponentially compared to (and underneath) the lightest state in the channel. Each new state requires a fit with two more parameters (the mass and $\langle 0 | O_j | n \rangle^2$), which in turn requires a fine lattice with many lattice points. At very short distance (order one lattice spacing) lattice discretization artifacts affect results. (Note that correlators like $C(t)$ probe long distances, even at small t .) I have not done direct calculations of spectra, and so my approach is more indirect and my results are tentative.

I will look at correlators with point sources and sinks, $O_j(x, t) = \bar{\psi}(x, t) \Gamma_j \psi(x, t)$. Lattice simulations usually do not use pointlike currents as interpolating fields because they do not couple to low states as well as more extended operators, and parameters of the lowest states are usually the goals of the simulation. However, for our purposes, it will be interesting to keep this simple form, and look at Γ_j 's which are chiral partners.

In contrast to usual lattice simulations, all results presented here are qualitative.

II. EXACT RESULTS FROM OVERLAP ACTIONS

The calculations presented here are done with overlap [19] fermions. This lattice discretization preserves a lattice version of exact chiral symmetry at nonzero lattice spacing, without flavor doubling, making it particularly useful for addressing questions associated with chiral symmetry. The following properties of overlap actions are relevant to this work:

The eigenmodes of any massless overlap operator are located on a circle in the complex plane of radius x_0 with a center at the point $(x_0, 0)$. The corresponding eigenfunctions are either chiral (for the eigenmodes with real eigenvalues located at $\lambda = 0$ or $\lambda = 2x_0$) or nonchiral and paired; the two eigenvalues of the paired nonchiral modes are complex conjugates.

The massive overlap Dirac operator for bare quark mass m is conventionally defined to be

$$D(m) = \left(1 - \frac{m}{2x_0}\right) D(0) + m \tag{3}$$

and it is also conventional to define the propagator so that the chiral modes at $\lambda = 2x_0$ are projected out,

$$\hat{D}^{-1}(m) = \frac{1}{1 - m/(2x_0)} \left(D^{-1}(m) - \frac{1}{2x_0} \right). \tag{4}$$

The contribution to the propagator of a single (positive chirality) zero mode in the basis where $\gamma_5 = \text{diag}(1, -1)$ is

$$\hat{D}(m)^{-1} = \frac{1}{m} \begin{pmatrix} |j+\rangle \langle j+| & 0 \\ 0 & 0 \end{pmatrix}. \tag{5}$$

Nonzero eigenvalue eigenmodes of $D(0)^\dagger D(0)$ are also chirality eigenmodes. The j th pair of nonchiral modes contributes a term to the propagator

$$\hat{D}(m)_j^{-1} = \begin{pmatrix} \alpha_j |j+\rangle \langle j+| & -\beta_j |j+\rangle \langle j-| \\ \beta_j |j-\rangle \langle j+| & \alpha_j |j-\rangle \langle j-| \end{pmatrix}, \quad (6)$$

where, using $D(0)^\dagger D(0)|jh\rangle = \lambda_j^2 |jh\rangle$ for chirality h , $\mu = m/(2x_0)$, and $\epsilon_j = \lambda_j/(2x_0)$, the entries are

$$\alpha_j = \frac{1}{2x_0} \frac{\mu(1 - \epsilon_j^2)}{\epsilon_j^2 + \mu^2(1 - \epsilon_j^2)} \quad (7)$$

$$\beta_j = \frac{1}{2x_0} \frac{\epsilon_j \sqrt{1 - \epsilon_j^2}}{\epsilon_j^2 + \mu^2(1 - \epsilon_j^2)}. \quad (8)$$

(The eigenmodes of $D(0)$ have eigenvalues $2x_0(\epsilon_j^2 \pm i\epsilon_j \sqrt{1 - \epsilon_j^2})$.) For a summary of these (and other) useful formulas, see Ref. [20] (for the special case $x_0 = 1/2$).

What is important about these well-known results is their application to correlators expressing the sum and difference of opposite parity channels:

$$C_{\pm\Gamma}(x, x') \propto \text{Tr} \hat{D}^{-1}(m) \Gamma \Delta_{\pm} \Gamma \quad (9)$$

where

$$\Delta_{\pm} = \hat{D}^{-1}(m) \mp \gamma_5 \hat{D}^{-1}(m) \gamma_5 \quad (10)$$

The parity difference is particularly simple: it involves the sum combination, which because of the Ginsparg-Wilson relation [21] is equal to

$$\Delta_- = 2m(\hat{D}^{-1}(m))^\dagger \hat{D}^{-1}(m) \quad (11)$$

The volume-summed trace of Δ_- gives the Gell-Mann-Oakes-Renner (GMOR) relation. Eigenmode by eigenmode, Δ_+ and Δ_- can be evaluated directly from Eq. 6; the former contribution comes from the off-diagonal part of \hat{D}^{-1} while the latter contribution comes from the diagonal elements.

This decomposition makes no reference to any dynamics. Thus the parameter which differentiates between chiral symmetry and asymmetry is just the quark mass—it is the only chiral breaking parameter which is available. The ratio of a contribution of an eigenmode to the chiral-difference correlator to the chiral symmetric correlator scales roughly as m/λ_j . This is rather similar to continuum free-field behavior, with $\Delta_-(p) = m/p^2$, $\Delta_+(p) = \not{p}/p^2$. It is NOT the behavior seen for Wilson-like fermions, which have an explicit chiral-symmetry breaking term at large momentum, $D^{-1}(m) = m + i \sum_{\mu} \gamma_{\mu} \sin(p_{\mu}a)/a + 2a \sum_{\mu} \sin^2(p_{\mu}a/2)$. Staggered fermion correlators entangle parity partners in a way I do not know how to present simply.

Naively, this means that, unless the $m \rightarrow 0$ limit is singular, parity difference correlators will go to zero with the quark mass. However, we have to be more careful [23], because the eigenmode density $\rho(\lambda)$ diverges in the ultraviolet as λ^3 . Mode sums generally require subtraction: high eigenmodes do contribute to all susceptibilities. For example, the pseudoscalar susceptibility (time integral of $C_j(t)$ for $\Gamma_j = \gamma_5$) is

$$\chi_{\pi} = \frac{1}{V} \sum_{x,y} \langle \pi^a(x) \pi^a(y) \rangle = \int d\lambda \rho(\lambda) \frac{1}{\lambda^2 + m^2} \quad (12)$$

and the scalar susceptibility is

$$\chi_{a_0} = \frac{1}{V} \sum_{x,y} \langle a_0^a(x) a_0^a(y) \rangle = \int d\lambda \rho(\lambda) \frac{\lambda^2 - m^2}{(\lambda^2 + m^2)^2} \quad (13)$$

For either susceptibility, it is necessary to break the integral over λ into two parts, one for the low modes $0 < \lambda < \Lambda_c$ where $\Lambda_c \gg m$, and one for the high modes. The low modes give the Banks-Casher relation for χ_{π} , $\chi_{\pi} = \rho(0)/(\pi m) + \dots$. The high frequency part of the integral must be subtracted twice,

$$\chi_{\pi} = \frac{1}{m} \left(\int_0^{\Lambda_c} d\lambda \rho(\lambda) \frac{m}{\lambda^2 + m^2} \right) + \gamma_0 + \gamma_2 m^2 + m^4 K_{\pi}(\Lambda_c, m). \quad (14)$$

The scalar susceptibility has a similar behavior, except that there is no contribution from $\lambda = 0$ [22]. For overlap fermions, the GMOR relation is exact,

$$\chi_\pi = \frac{2}{m} \langle \bar{\psi}\psi(m) \rangle \quad (15)$$

and the scalar susceptibility is

$$\chi_{a_0} = 2 \frac{d}{dm} \langle \bar{\psi}\psi(m) \rangle, \quad (16)$$

so that the expansion coefficients in the expansions for χ_π and χ_{a_0} are related. In the difference $\chi_\pi - \chi_{a_0}$ the contribution from the chiral condensate (which comes from eigenmodes near $\lambda = 0$) survives and dominates in the $m \rightarrow 0$ limit. The mass-independent term in $\chi_\pi - \chi_{a_0}$ cancels. The chiral sum $\chi_\pi + \chi_{a_0}$ retains the high- λ dependent γ_0 coefficient. The terms proportional to positive powers of m vanish in the massless limit in either case. What is true for an integral is not necessarily true for an integrand, but it is a plausible assumption to expect that chiral difference correlators themselves will receive large contributions only from low eigenmodes, while high eigenmodes will contribute strongly to chiral sum correlators. For example, one might expect that the low modes would dominate the pseudoscalar correlator: then [24],

$$C_{PS}(x, x') = \left\langle \left\{ \sum_\lambda \langle j, \lambda, x | j, \lambda, x \rangle \frac{1}{\lambda^2 + m^2} \langle j, \lambda, x' | j, \lambda, x' \rangle \right\} \right\rangle \quad (17)$$

This reasoning is dangerous because of the UV divergence of $\rho(\lambda)$, but it can be tested by simulation.

Zero modes decouple from $C_+(x, x')$. They make a large contribution to $C_-(x, x')$. This is not surprising: zero modes are chiral. They will, however, considerably distort chiral-difference correlators in small volumes.

III. EXAMPLES

I have done a set of quenched spectroscopy runs using a particular implementation of the overlap operator [25] with HYP [26] gauge connections. Eigenmodes of the Dirac operator are computed using the conjugate gradient algorithm of Ref. [27]. These studies are done on a small data set of quenched configurations. It has 20 16^4 lattices generated with the Wilson gauge action at coupling $\beta = 6.1$, corresponding to a lattice spacing of about 0.09 fm. These lattices have the same lattice spacing and quark masses as were used in a large scale matrix element simulation [28], so all necessary hadron masses and matrix elements are in principle known. I have computed the lowest 20 eigenmodes of $D(0)^\dagger D(0)$ and recoupled them into eigenmodes of D : there are N_0 chiral zero modes and $2(20 - N_0)$ nonchiral paired modes. Eigenmodes of the overlap Dirac operator whose eigenvalue is less than around 500 MeV have been computed. The spectrum of the imaginary part of the eigenvalue is shown in Fig. 1. The energy is inferred from the lattice data assuming an inverse lattice spacing of 2200 MeV. I compute hadron correlators using full quark propagators, and several kinds of quark propagators built of truncated mode sums: quark propagators with only zero modes, propagators without zero modes, and propagators from which the lowest 10 or 20 eigenmodes of $D^\dagger D$ have been excluded.

I will show results corresponding to bare quark masses in lattice units of $am_q = 0.020$, which is about half the strange quark mass. A meson made of a pair of $am_q = 0.020$ quarks is an approximation to the physical kaon. Results for other small quark masses are similar. At higher quark masses (above $am_q = 0.050$ or $m_q \geq 2.5m_s$) the qualitative features I present do no longer occur. Pictures shown in Refs. [2, 3] show that low modes cease to contribute a dominant part of any correlator.

Because these simulations are done in finite volume, and in quenched approximation, some channels have contributions from zero modes of the Dirac operator. These contributions would not be present in infinite volume. In other channels these modes are absent.

A. “Spectroscopic” correlators with point sources

I begin first with correlators $C(t)$ of Eq. 1. Results for pseudoscalars and scalars are shown in Fig. 2. Panel (a) shows the sum of pseudoscalar and scalar correlators. Note the complete saturation of the correlator for $t > 5$ by low modes, and the essentially complete saturation of the correlator by high modes at shorter distances. The pionic contribution to the correlator, using $\langle 0 | \bar{\psi}\gamma_5\psi | PS \rangle = m_{PS}^2 f_{PS} / (2m)$, (with the fitted parameters m_{PS} and f_{PS} from Ref. [28]) is superimposed. The low modes make up the bulk of the pion’s contribution to the correlator.

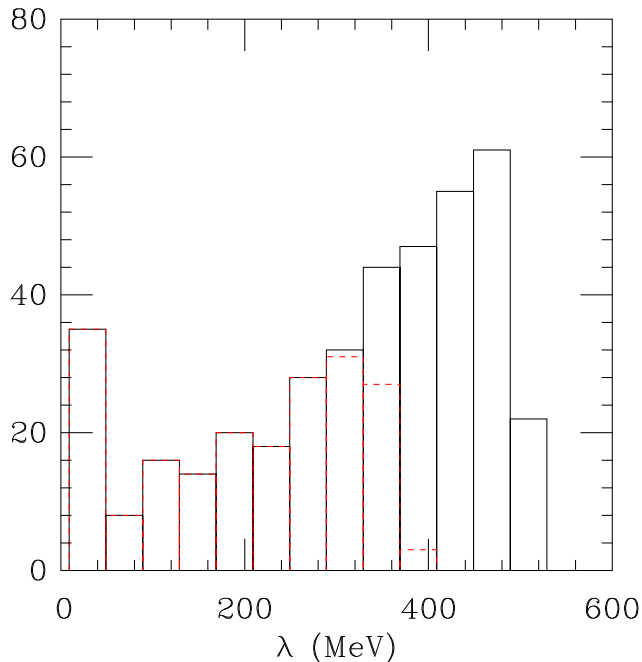


FIG. 1: Histogram of eigenvalues of the Dirac operator of eigenmodes recorded for this study. The peak at the lowest box contains all zero modes. The black solid lines curve shows the distribution of the twenty lowest eigenmodes of $D^\dagger D$, while the red dashed lines separate the distribution of ten modes.

Panel (b) shows the difference of pseudoscalar and scalar correlators. This signal is heavily influenced by zero modes, so that while low modes again contribute a “pion-like” signal, most of this contribution involves at least one zero mode. High eigenmodes make a negligible contribution to the correlator at any time separation.

The axial-scalar $(\gamma_0\gamma_5 - \gamma_5\gamma_0) \pm (\gamma_0 - \gamma_0)$ combination shows similar behavior (panels (c) and (d)). The axial vector current decouples from the Goldstone mode in the chiral limit, and this is reflected in the “sum” correlator by a slower saturation of the pion contribution to the correlator by low modes. Again, the bulk of the signal at small time steps comes from high modes. High modes do not contribute to the chiral difference.

Vector and axial combinations (Fig. 3, panels (a) and (b)) lack any single state which is dominated by low modes. High modes again make a tiny contribution to the chiral-asymmetry channel, and saturate the signal in the chirally symmetric channel. The absolute size of the correlators in the two channels is quite different at short distances.

The correlator $C_+(t)$ is almost two orders of magnitude larger than $C_-(t)$ in the vector-axial channel, and almost three orders of magnitude larger in the pseudoscalar-scalar channel. This is not a direct observation that the spectrum of quenched QCD is parity-doubled at high excitation. However, this is the “raw data” from which masses are extracted, so it is likely that any fit to it for masses will produce parity symmetric results.

Perhaps direct comparisons, in Fig 4, are clearer. Panel (a) shows the pseudoscalar and scalar correlators; I have subtracted the measured pion contribution from the pseudoscalar channel. Panel (b) shows the vector and axial vector correlators. The correlators $C_j(t)$ defined in Eq. 1, where Γ_j are parity partners (γ_5 and 1, γ_i and $\gamma_i\gamma_5$), become equal for t less than about 0.2 fm.

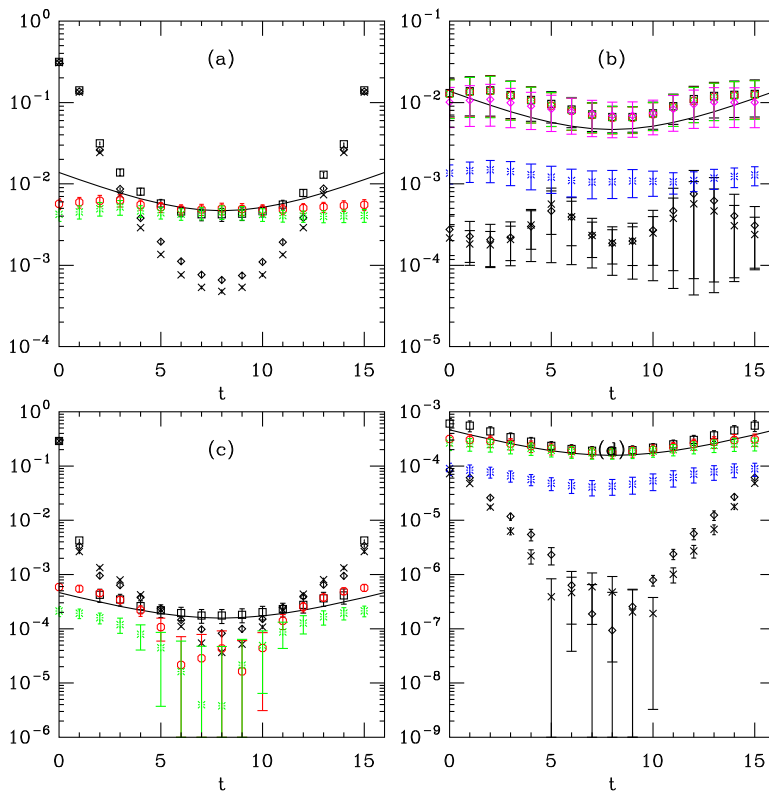


FIG. 2: Combinations of point-to-point pseudoscalar and scalar ($\pi \pm a_0$) sum (a) and difference (b) correlators, and axial vector $\gamma_0 \gamma_5 - \gamma_0 \gamma_5$ and scalar $\gamma_0 - \gamma_0$ sums (c) and differences (d). The full correlators are shown by open squares. Their approximation by restricted-mode quark propagators with 20 lowest modes (red octagons) or 10 lowest modes (green bursts). Crosses and diamonds show the contribution to the correlator from quark propagators with 20 and 10 low modes excluded. The curve is the contribution to the correlator from the pion, using its measured mass and decay constant from a different simulation. In panels (b) and (d) the contribution of the lowest 20 eigenmodes with zero modes excluded is shown in blue fancy diamonds, and the pure zero mode contribution (magenta fancy crosses) is shown in (b).

B. Point-to-point correlators

One can also compute point-to-point correlators (Eq. 2). The short distance, parity-summed correlators receive little contribution from low eigenmodes. That their ratios approach unity at small x is just asymptotic freedom. However, this is a confining theory: the spectrum of quenched QCD consists of zero width resonances plus quenched artifacts (mostly associated with eta prime hairpins). A more correct statement of what is seen is that the resonances which make up the low- x part of the sum correlators receive little contribution from low modes. Results are shown in Fig. 5.

The parity difference correlators vanish at low x . Low eigenmodes (including zero modes) dominate the correlators

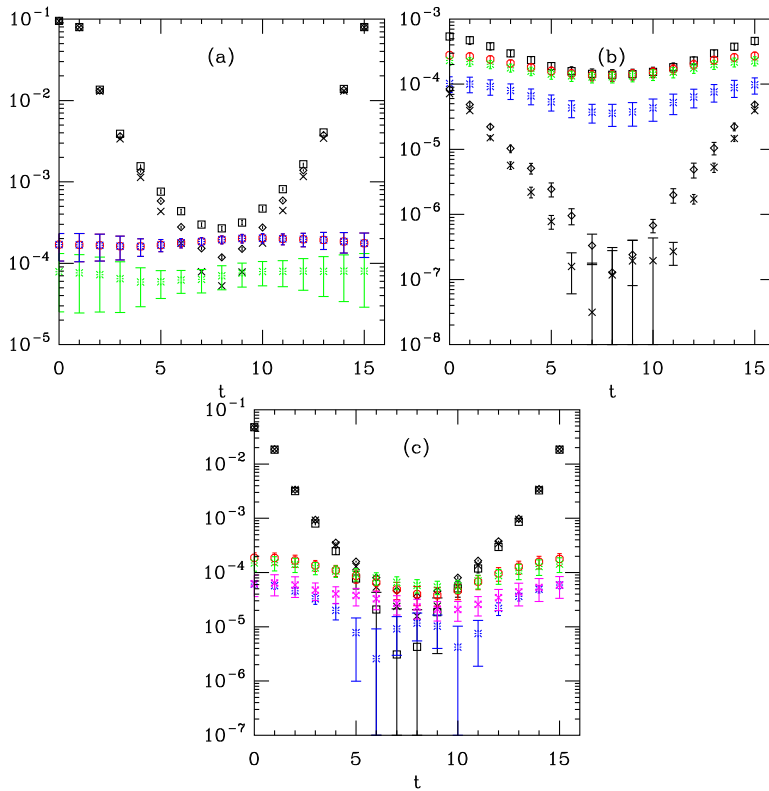


FIG. 3: Point-to-point $(\gamma_i - \gamma_i) \pm (\gamma_i \gamma_5 - \gamma_i \gamma_5)$ (rho plus/minus a_1) correlator: (a) sum, (b) difference, and (c) tensor or a_2 correlator $(\gamma_i \gamma_j - \gamma_i \gamma_j)$. Full correlators are shown as black squares, and their approximation by restricted-mode quark propagators with 20 lowest modes (red octagons), 10 lowest modes (green bursts), and pure zero mode contribution (magenta fancy crosses) are also shown. The contribution of the lowest 20 eigenmodes with zero modes excluded are blue fancy diamonds. Crosses and diamonds show the contribution to the correlator from quark propagators with 20 and 10 low modes excluded.

at large x , where the lightest states in the channel appear. Alternatively, the strong attraction seen at large x in the pseudoscalar channel comes almost entirely from eigenmodes below 500 MeV.

In the absence of reliable spectroscopy calculations, we can roughly quantify the “breakpoint” between low and high mode contributions by considering the contribution of a single resonance of mass m to one of these ratios. This curve is proportional to the ratio $x^5 K(m, x)$, where $K(m, x)$ is the free field propagator for a particle of mass m . A family of curves of varying masses (in lattice units) is shown in Fig. 6; the height has been rescaled as m^2 to produce a plateau of maxima. What is important from this picture is not the height of the peaks, it is their location. If we compare the high eigenmode and full propagator curves in Fig 5(a) and (c), we see that they separate at a lattice distance of about 5 units. Any resonance with a lattice mass lighter than $am_H < 0.75$ would make its peak contribution at larger x . This mass is about 1700 MeV, and is the rough dividing point between hadrons built dominantly of chiral sensitive modes and ones which are not, for quenched QCD. (Again, recall that the inverse lattice spacing of these

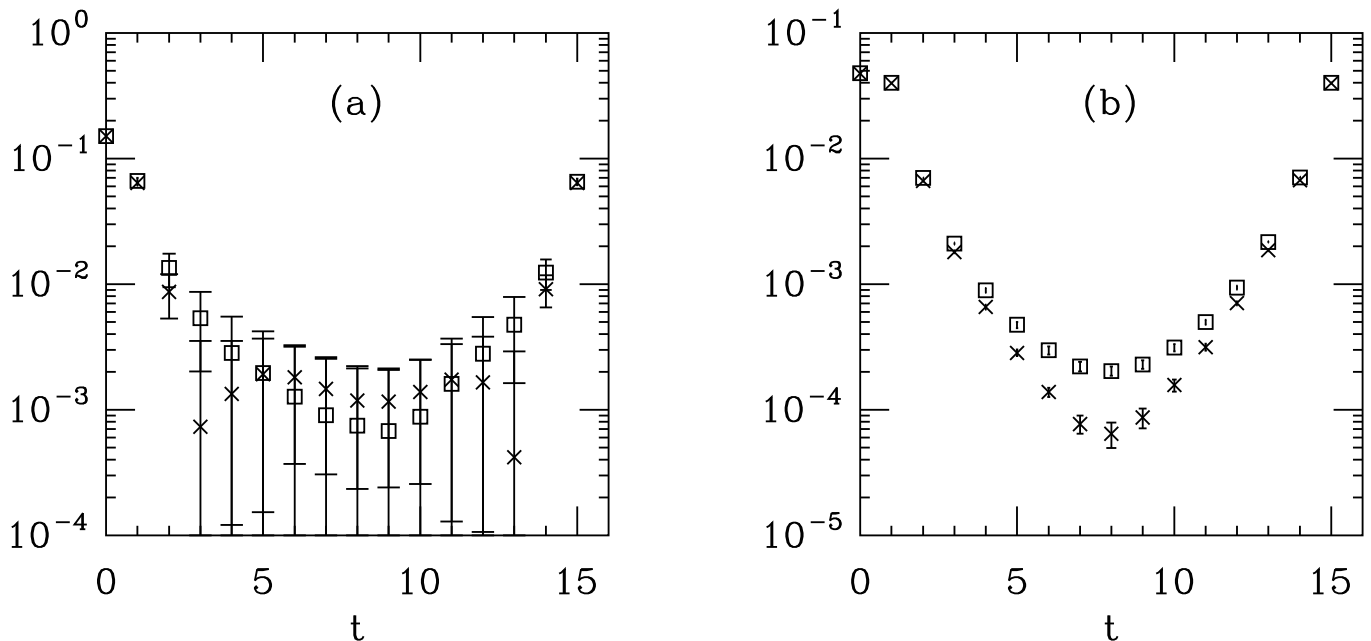


FIG. 4: (a) Point-to-point $(\gamma_5 - \gamma_5)$ correlator, with pionic contribution removed (squares) and $1-1$ (crosses) correlators at bare mass $am_q = 0.02$. (b) point-to-point $(\gamma_i - \gamma_i)$ (squares) and $(\gamma_i \gamma_5 - \gamma_i \gamma_5)$ (crosses) correlators

simulations, above which discretization effects dominate physics, is about 2.2 GeV). Swanson's estimate [17] of 2.5 GeV for the crossover corresponds to $ma \simeq 1.1$, but given the roughness of either estimate, I would not take the difference seriously.

Finally, we show in Fig. 7 the saturation of the amplitude for chirality flipping proposed by Ref. [29] and computed on the lattice in Ref. [6],

$$R^{NS}(x) = \frac{\Pi_\pi(x) - \Pi_{a_0}(x)}{\Pi_\pi(x) + \Pi_{a_0}(x)}, \quad (18)$$

using complete quark propagators and high-eigenmode truncations. Clearly the high eigenmodes make a tiny contribution to R^{NS} ; it is the low modes that are strongly influenced by chirality mixing interactions.

IV. CONCLUSIONS

Lattice simulations in which contributions to quark propagators from low and high eigenvalue eigenmodes of the Dirac operator are separated identify the following qualitative features of light-quark mesons in quenched QCD: Low eigenmodes make a large contribution to the pion propagator. They are responsible for the strong long-distance attractive interaction seen in the pseudoscalar channel. Low eigenmodes of the Dirac operator make a small contribution to the short distance part of correlators (where excited states contribute). These are the eigenmodes which determine the quark condensate via the Banks-Casher relation, as well as eigenmodes at the QCD scale" (a few hundred MeV). This implies that valence quarks in high-lying states decouple from the condensate.

I have not directly observed parity doubling at high excitation in the meson spectrum, but lattice correlation functions in parity-partner channels (from which fits to masses would be performed) are equal at a part in 10^{3-4} at short distances. Point-to-point correlators suggest that hadrons of mass above 1.7 GeV are insensitive to low Dirac eigenmodes. Low modes do not contribute to the tensor meson correlator.

Perhaps these results can be used to constrain phenomenological models of hadron structure. Results such as Fig. 2(a) suggest that it might be profitable for lattice calculations done at small quark mass to exploit low eigenmodes of the Dirac operator in simulations.

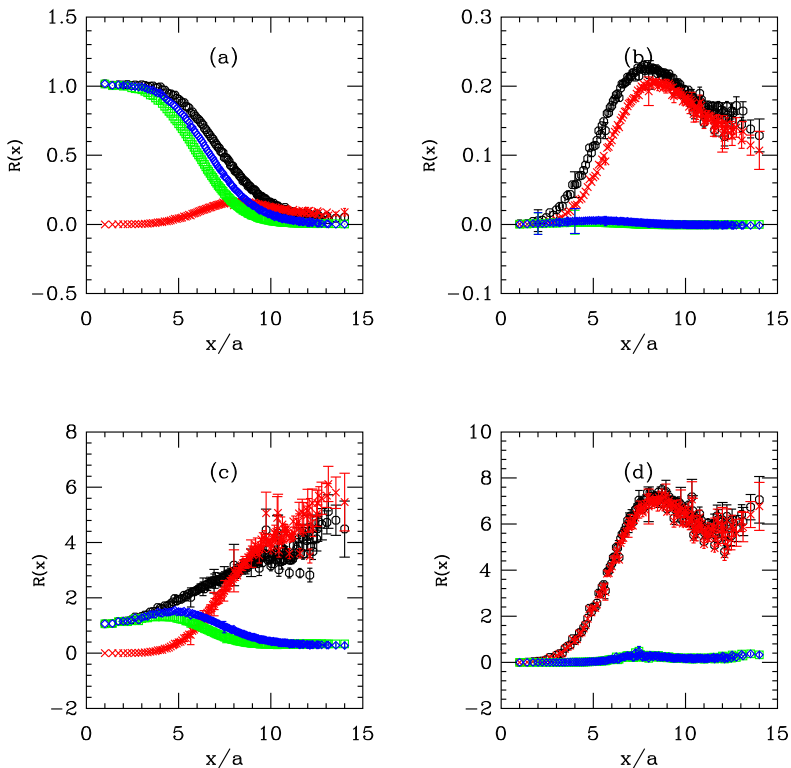


FIG. 5: Point-to-point $(\gamma_\mu - \gamma_\mu) \pm (\gamma_\mu \gamma_5 - \gamma_\mu \gamma_5)$ vector-axial vector sum (a) and difference (b), and $(\gamma_5 - \gamma_5) \pm (1 - 1)$ pseudoscalar-scalar sum (c) and difference (d), normalized by free field vector and scalar currents, Full correlators are shown in black and approximation by restricted-mode quark propagators with 20 lowest modes (red crosses) and contributions from propagators containing all but the lowest 20 (blue diamonds) or 10 (green squares) modes.

Acknowledgments

This work arose through discussions with Leonid Glotzman, and I am grateful to him for numerous conversations, correspondence, and encouragement. This project was begun while I was a guest at the Max Planck Institute for Physics and Astrophysics, Munich, and I appreciate for that institution's hospitality. This work was supported by the US Department of Energy.

-
- [1] V. A. Novikov, M. A. Shifman, A. I. Vainshtein and V. I. Zakharov, Nucl. Phys. B **191**, 301 (1981).
 [2] T. DeGrand and A. Hasenfratz, Phys. Rev. D **64**, 034512 (2001) [arXiv:hep-lat/0012021].

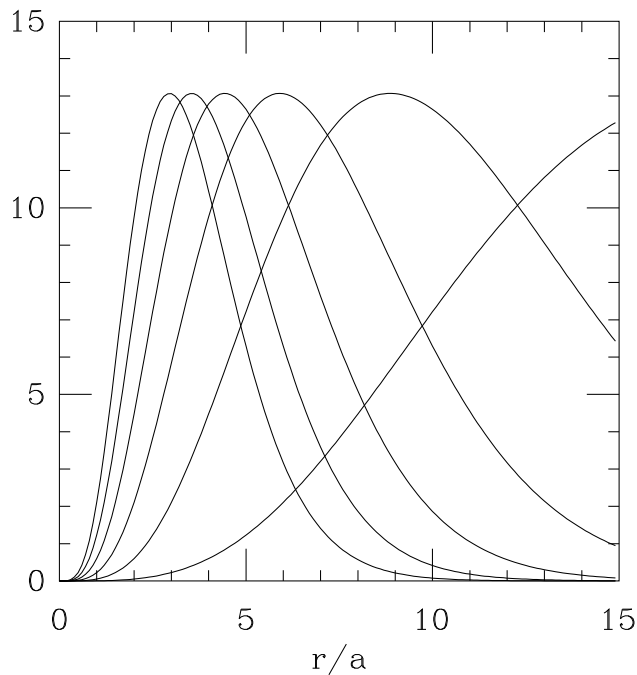


FIG. 6: $x^5 K(x)$, the contribution of a resonance of mass m to one of the point-to-point correlator ratios. The peaks correspond to lattice masses (from left to right) of $m_H a = 1.5, 1.25, 1.0, 0.75, 0.5$, and 0.25 (the peak of the last curve lies outside the graph).

- [3] T. DeGrand, Phys. Rev. D **64**, 094508 (2001) [arXiv:hep-lat/0106001].
- [4] T. DeGrand and U. M. Heller [MILC collaboration], Phys. Rev. D **65**, 114501 (2002) [arXiv:hep-lat/0202001].
- [5] T. Banks and A. Casher, Nucl. Phys. B **169**, 103 (1980).
- [6] P. Faccioli and T. A. DeGrand, arXiv:hep-ph/0304219.
- [7] P. Faccioli and T. A. DeGrand, arXiv:hep-lat/0309129.
- [8] T. D. Cohen and L. Y. Glozman, Phys. Rev. D **65**, 016006 (2002) [arXiv:hep-ph/0102206].
- [9] L. Y. Glozman, Phys. Lett. B **541**, 115 (2002) [arXiv:hep-ph/0204006].
- [10] L. Y. Glozman, Prog. Part. Nucl. Phys. **50**, 247 (2003) [arXiv:hep-ph/0210216].
- [11] T. D. Cohen and L. Y. Glozman, Int. J. Mod. Phys. A **17**, 1327 (2002) [arXiv:hep-ph/0201242].
- [12] L. Y. Glozman, arXiv:hep-ph/0304087.
- [13] S. R. Beane and M. J. Savage, Phys. Lett. B **556**, 142 (2003) [arXiv:hep-ph/0212106].
- [14] L. Y. Glozman, arXiv:hep-ph/0309334.
- [15] S. R. Beane, Phys. Rev. D **64**, 116010 (2001) [arXiv:hep-ph/0106022].
- [16] M. Golterman and S. Peris, Phys. Rev. D **67**, 096001 (2003) [arXiv:hep-ph/0207060].
- [17] E. S. Swanson, arXiv:hep-ph/0309296.
- [18] T. Schafer and E. V. Shuryak, Rev. Mod. Phys. **70**, 323 (1998) [arXiv:hep-ph/9610451].
- [19] H. Neuberger, Phys. Lett. **B417**, 141 (1998) [hep-lat/9707022], Phys. Rev. Lett. **81**, 4060 (1998) [hep-lat/9806025].
- [20] R. G. Edwards, U. M. Heller and R. Narayanan, Phys. Rev. **D59**, 094510 (1999) [hep-lat/9811030].
- [21] P. H. Ginsparg and K. G. Wilson, Phys. Rev. **D25**, 2649 (1982).
- [22] A. V. Smilga and J. Stern, Phys. Lett. B **318**, 531 (1993).
- [23] H. Leutwyler and A. Smilga, Phys. Rev. D **46**, 5607 (1992).
- [24] M. Golterman and Y. Shamir, arXiv:hep-lat/0306002.
- [25] T. DeGrand [MILC collaboration], Phys. Rev. D **63**, 034503 (2001) [hep-lat/0007046].
- [26] A. Hasenfratz and F. Knechtli, Phys. Rev. D **64**, 034504 (2001) [arXiv:hep-lat/0103029].

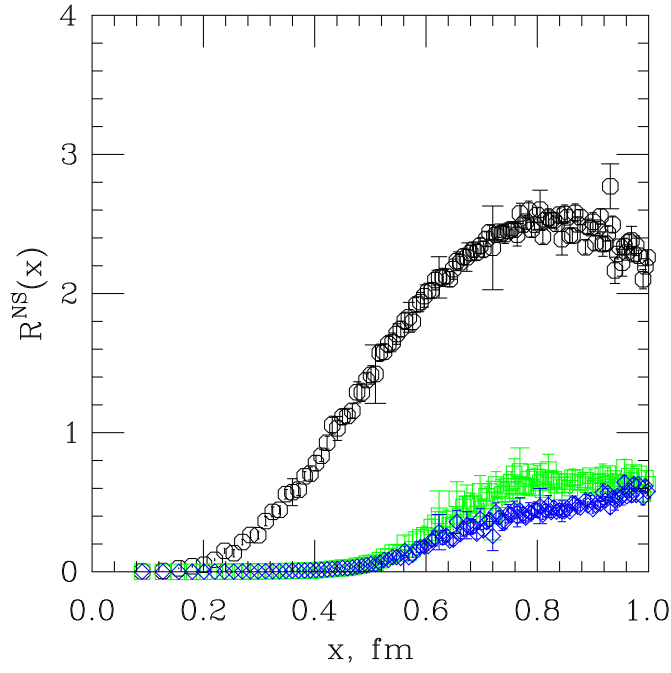


FIG. 7: $R^{NS}(x)$ as defined in Eq. 18 and its contribution from propagators from which the lowest 20 (blue diamonds) and 10 (green squares) eigenmodes of $D^\dagger(0)D(0)$ are excluded.

- [27] See B. Bunk, K. Jansen, M. Lüscher, and H. Simma, unpublished DESY report (1994); T. Kalkreuter and H. Simma, *Comput. Phys. Commun.* **93**, 33 (1996) [hep-lat/9507023].
- [28] T. DeGrand, arXiv:hep-lat/0309026.
- [29] P. Faccioli, arXiv:hep-ph/0211383.